Computing Molecular Weight Distribution in Commercial Synthesis of PTMEG: Dynamic Reactor Modeling of $HFSO_3$ Initiated Polymerization of THF

Richard D Skeirik

Independent Consultant, 873 E Baltimore Pike #742, Kennett Square, PA 19348 United States
Telephone: 610 925 0312
Email address: richardskeirik@richardskeirik.com

Abstract[a]

Synthesis of Polytetramethylene ether glycol (PTMEG) by fluorosulfonic acid (FSA) initiated polymerization of bulk tetrahydrofuran (THF) accounts for perhaps 108,000 mt/yr or 20% of 2012 world capacity of this component of spandex fiber and elastomers. A dynamic batch kinetic reactor model of this system, tracking each individual chain length, can produce a full molecular weight distribution (MWD) and reproduce measured compositions and average molecular weight. The model opens a new approach to optimize conversion, average molecular weight, and MWD in this mature process with the potential to improve quality, reduce cost, make higher value products, and reduce environmental impact. Because FSA's fluorosulfate ion reacts, forming three variants of both chain ends, the model tracks nine chain populations up to a degree of polymerization of 100. These fluorosulfate ion reactions result in chain termination and chain transfer to initiator, which shift the MWD away from the geometric progression that would result in their absence. For this reason, neither lumped models nor the lone applicable analytical formula for MWD are accurate for this synthesis. A dynamic lumped batch model predicts average molecular weight well, but gives the wrong monomer conversion vs. time. Both models can be easily adapted to dynamic CSTR or semi-

---

[a] Abbreviations used: **PTMEG:** Polytetramethylene ether glycol; **FSA:** fluorosulfonic acid; **THF:** tetrahydrofuran; **MWD:** molecular weight distribution; **DAS:** psuedo end group and pseudo component dialkyl sulfate; **DP:** degree of polymerization; **ODE**: ordinary differential equation.

batch form, and have value for process design and optimization. Using its ability to predict average molecular weight, the lumped model can be incorporated into a flowsheet model and used to evaluate process layout, optimization or control options; which can be subsequently be confirmed or refined by solution of the detailed model. The detailed model can be used for recipe or control design, for optimization where modeling or existing equipment already define a process layout, or as an inferential estimator supplementing lab measurements for control.

CES Keywords: Reaction engineering
Polymerization
Kinetics
Molecular weight distribution
Polytetramethylene ether glycol
Fluorosulfonic acid

1 Introduction

Polytetramethylene ether glycol (**PTMEG**), the di-hydroxy terminated oligomer ($H-[O(CH_2)_4]_n-OH$) of tetrahydrofuran (**THF**), is an industrially important polyether (Pruckmayr et al., 2000) that imparts stretch in spandex fibers and flexibility in elastomeric polyurethanes. PTMEG is commercially produced mainly in three ways: by reaction of THF in bulk liquid using fluorosulfonic acid (**FSA**) as initiator (Pruckmayr and Wu, 1978); by the reaction of THF with an immobilized acid catalyst/initiator (Dorai et al., 1992); or by reaction of THF with acetic anhydride/clay (Mueller et al., 1980.)

BASF, the world's largest producer, in 2012 expanded its global PTMEG capacity to 250,000 metric tons/year (mt/yr) (IHS Chemical Week, 2012.) In 2007, DuPont's PTMEG product line was 90,000 mt/yr (Bryner, 2007.) In 2010, Invista's LaPorte, TX (USA) plant could produce 41,000 mt/yr (Chemical Week, 2010.) These producers use immobilized acid processes. Of China's 2008 capacity of 160,000 mt/yr, 60,000 comes from BASF's Caojing plant (China Chemical Reporter, 2010), China's largest, and 20,000 mt/yr comes from the Jilin Qianguo Refinery using an advanced process from America (China Chemical Reporter, 2005.) The remaining 100,000 mt/yr comes from smaller, older plants (Zejiang and Hui, 2010.) Lynondell offers PTMEG, last reported to be tolled through two older 14,000 mt/yr US plants (Paint & Coatings Industry Magazine, 2002; Chemical Week, 1999.) While industry reports rarely disclose the technology used in PTMEG plants, a significant fraction of world PTMEG is still manufactured by FSA initiation. Of the 543,000 mt/yr cited above, 108,000 mt/yr, or about 20% of world capacity, appears to use FSA initiation.

The immobilized acid and the anhydride/clay technologies remain mostly proprietary to the inventing companies, and they have published little about it. In contrast, over decades chemists have published many studies of various acid initiated polymerizations, including a number of studies defining some of the kinetic rate constants. Yet there do not appear to be any published reactor models for this system. For design or optimization of a commercial process, models have obvious value. The model presented here fills this void. Based on published batch polymerization experiments, two dynamic reactor models were developed: a lumped model using approximate kinetics, but promising integration into larger flowsheet studies, and a distributed model which accurately models the kinetics and predicts the complete molecular weight distribution, with corresponding cost in complexity and computation. The results presented here are limited to reproducing the batch experiments, but the model formulation can readily be adapted to continuous or semi-batch form.

2 Chemistry

The simplest chemistry of the acid initiated polymerization of THF is outlined in the review of Pruckmayr et al. (2000.)

$THF + H^{+} \rightleftarrows H\text{-}{}^{+}THF$ Activation, Oxonium Ion Formation (1)

$H\text{-}[O(CH_2)_4]_n\text{-}{}^{+}THF + THF \rightleftarrows H\text{-}[O(CH_2)_4]_{n+1}\text{-}{}^{+}THF$ Propogation/de (2)

Here ***[O(CH₂)₄]*** is the ring-opened THF monomer; a segment in the polyether chain. **$^{+}$THF** is used here to refer to the cyclic oxonium ion form of THF, still a closed ring, but capable of forming a third bond to the positively charged oxygen atom. THF polymerization is reversible, with higher temperatures increasingly favoring the reverse (depropagation) reaction. This results in a ceiling temperature of 83 ºC (Pruckmayr et al., 2000), above which no polymer will form. In this system, H^{+} is an initiator. It chemically combines with monomer to form the active polymerizing species, and so, absent chain transfer, there can be at most one chain for each H^{+} provided by the acid.

When first activated by the reaction of **equation (1)**, oxygen forms a third bond to hydrogen; creating a secondary oxonium ion. Once a second THF monomer adds by the reaction of **equation (2)**, the third bond changes to the carbon chain of a polyether segment: $O(CH_2)_4$; creating a tertiary oxonium ion. A hydrogen atom presents little steric hindrance compared to a polyether chain, and so there may be some difference in reactivity of the oxonium ion between the secondary and tertiary forms. Since there is no data to the contrary, it will reduce model complexity to make the reasonable assumption that the reactivity is the same. This means that the secondary oxonium ion product of equation (1) can be treated as a growing chain with a chain length of zero: $H\text{-}[O(CH_2)_4]_0\text{-}{}^{+}THF$. As shown later, when we use this assumption in a lumped model, it is impossible to treat the reaction in equation (1) as irreversible, because without knowing the concentration of the active chains with n=0, we cannot specifically exclude their reverse reaction while still including it for all the longer species within that lump.

2.1 FSA Reactions

The use of FSA to initiate the polymerization adds complexity to the system. FSA, a very strong acid, is used because it dissociates in the polymerizing mixture; something that weaker acids tend not to do. Pruckmayr and Wu (1978) showed that the $FSO_3{}^-$anion resulting from FSA dissociation attacks both ends of the propagating chains, forming chains terminated in other end groups besides OH and $^+$THF. These further react to create non-polyether groups embedded within chains. These reactions and their effects are at the heart of this study.

First, $FSO_3{}^-$ can attack the non-polymerizing OH end group, forming a sulfate end group. For clarity, the **functional groups/molecules that are involved in the reaction are shown with underscore**:

$$\underline{FSO_3{}^-} + \underline{H}\text{-}[O(CH_2)_4]_n\text{-}{}^+THF \rightarrow \underline{HO_3S}\text{-}[O(CH_2)_4]_n\text{-}{}^+THF + \underline{F^-} \qquad (3)$$

The resulting chain can still polymerize. Since HF tends not to dissociate in this system, the product F^- is likely to associate with a free proton, effectively consuming one equivalent of initiator (with subsequent effect on the MWD,)

$$F^- + H^+ \rightarrow HF \qquad (4)$$

$FSO_3{}^-$ can also attack the active polymerizing $^+$THF end group, opening the $^+$THF ring and forming a fluorosulfate end group, but in this case the active $^+$THF center is lost and the chain is dead, consuming one equivalent of initiator, and thus is a termination reaction:

$$H\text{-}[O(CH_2)_4]_n\text{-}\underline{{}^+THF} + \underline{FSO_3{}^-} \rightarrow H\text{-}[O(CH_2)_4]_{n+1}\text{-}\underline{OSO_2F} \qquad (5)$$

The fluorosulfate end sulfate end groups are also reactive. First, fluorosulfate can react with a hydroxyl end group, forming a dialkyl sulfate – a sulfate group embedded within the chain. This reaction, between two end groups inactive for chain growth, has no impact on the number of active polymerizing centers, nor on the amount of available initiating capacity.

$$\begin{gathered} H\text{-}[O(CH_2)_4]_n\text{-}\underline{OSO_2F} + \underline{H}\text{-}[(OCH_2)_4]_m\text{-}{}^{+}THF \rightarrow \\ H\text{-}[O(CH_2)_4]_n\text{-}\underline{OSO_2}\text{-}[O(CH_2)_4]_m\text{-}{}^{+}THF + \underline{HF} \end{gathered} \tag{6}$$

Last, the sulfate end group can attack a $^{+}$THF on another chain. This also creates an embedded dialkyl sulfate group and destroys an active center, while simultaneously liberating one equivalent of the initiator. This makes this reaction a chain transfer to initiator:

$$\begin{gathered} H\text{-}[O(CH_2)_4]_n\text{-}\underline{{}^{+}THF} + \underline{HOSO_2}\text{-}[O(CH_2)_4]_m\text{-}{}^{+}THF + \rightarrow \\ HO\text{-}[O(CH_2)_4]_{n+1}\text{-}\underline{OSO_2}\text{-}[O(CH_2)_4]_m\text{-}{}^{+}THF + \underline{H^{+}} \end{gathered} \tag{7}$$

While reactions involving a hydroxyl end group should not affect chain growth or resulting oligomer properties, the reactions that involve the active $^{+}$THF can affect growth, molecular weight and distribution, and oligomer properties, as can the liberation of F^{-} with subsequent reaction to form HF. Thus, a comprehensive model must account for these reactions.

Before this can be modeled, two issues must be accounted for. First, the coupling of chains through the formation of alkyl sulfate linkages appears to greatly complicate the chemistry and the resulting MWD. Luckily this will be resolved by considering the effect of the customary downstream processing of the polymerization mixture. Second, reactions which involve one specific end group are indifferent to the length of the chain or the end group on the opposite end. Considering the various end groups formed in the FSA chemistry, there are additional combinations of molecules which can participate in any one of these reactions. These are addressed in turn below.

2.2 Downstream Water Wash

The customary process step downstream of the polymerization is a water extraction (Pruckmayr et al., 2000). Among other functions, water hydrolyzes the sulfate and fluorosulfate links to the polyether chains, yielding OH groups on the ends of all polyether segments, and liberating H_2SO_4 or HF.

2.3 Pseudo End Groups and Component

From a reaction perspective during the polymerization, the embedded dialkyl sulfate group is similar to any other non-polymerizing end group, because it ends a polyether chain segment and prevents further polymerization of that end. It differs because it is bound to, and provides the end for, two chains, not one. But since the embedded dialkyl sulfate is hydrolyzed at both chain junctions, and the polyether segments are liberated with hydroxyl ends, the resulting MWD after water extraction is exactly the same as if the two chains each had their own hydrolyzable, non-polymerizing end group. From a process perspective, the only goal is to account for polyether chains as they exist after water extraction, and we can achieve this result by treating these dialkyl sulfate reactions as if two separate, unconnected, non-polymerizing end groups are created by the reaction. This pseudo end group is called here **DAS**.

Knowing this, we can simplify the reactions of **equation (6)** and **(7)**, using the DAS end group and separately accounting for the two chains, which in reality are linked by a dialkyl sulfate bond. Pruckmayr and Wu (1978) reported the relative concentration of dialkyl sulfate linkages over time, and it would be helpful to model this for model validation. We can do this by creating a pseudo-component, simply called DAS, which represents this group. We can account for this simply as if it were a separate product of the dialkyl sulfate formation reactions:

$$H\text{-}[O(CH_2)_4]_n\text{-}\underline{OSO_2F} + \underline{H}\text{-}[O(CH_2)_4]_m\text{-}{}^{+}THF \rightarrow$$
$$H\text{-}[O(CH_2)_4]_n\text{-}\underline{DAS} + \underline{DAS}\text{-}[O(CH_2)_4]_m\text{-}{}^{+}THF + \underline{HF} + DAS \tag{6a}$$

$$H\text{-}[O(CH_2)_4]_n\text{-}\underline{{}^{+}THF} + \underline{HOSO_2}\text{-}[O(CH_2)_4]_m\text{-}{}^{+}THF + \rightarrow H\text{-}[O(CH_2)_4]_{n+1}\text{-}\underline{DAS} +$$
$$\underline{DAS}\text{-}[O(CH_2)_4]_m\text{-}{}^{+}THF + \underline{H^+} + DAS \tag{7a}$$

2.4 Additional Reaction Combinations

Examining the reactions in **equation (3), (5), (6a), and (7a),** we can see that a number of variations in chain ends will exist in this reaction system. Any chain having one $^{+}$THF end group can participate in the reaction of equation (5) or (7a). Any chain with one OH end group can participate in the reaction of equation (3) or (6a). Any chain having one fluorosulfate end group can participate in the reaction of equation (6a). Any chain having a sulfate end group can participate in the reaction of equation (7a).

Using a curly brace to show the three possible end groups, all the reactions taking place, including the DAS simplification, are shown below and in Schema (1):

$$HFSO_3 \rightleftarrows H^+ + FSO_3{}^-$$

FSA Dissociation (8)

$$HF \rightleftarrows H^+ + F^-$$

HF Association *(9)*

$$THF + H^+ \rightarrow H-[(CH_2)_4O]_0 - {}^+THF$$

Initiation *(10)*

$$\left.\begin{matrix}H-\\HOSO_2-\\DAS-\end{matrix}\right\}\text{-}[O(CH_2)_4]_n - {}^+THF + THF \rightleftarrows \left.\begin{matrix}H-\\HOSO_2-\\DAS-\end{matrix}\right\}\text{-}[O(CH_2)_4]_{n+1}\text{-}{}^+THF$$

Propagation, depropagation *(11)*

$$\underline{FSO_3{}^-} + \underline{H}\text{-}[O(CH_2)_4]_n\text{-}\left\{\begin{matrix}-{}^+THF\\-O_2SOF\\-DAS\end{matrix}\right. \rightarrow \underline{HOSO_2}\text{-}[O(CH_2)_4]_n\text{-}\left\{\begin{matrix}-{}^+THF\\-O_2SOF\\-DAS\end{matrix}\right. + \underline{F^-}$$

FSO3 attack on OH *(12)*

$$\left.\begin{matrix}H-\\HOSO_2-\\DAS-\end{matrix}\right\}\text{-}[O(CH_2)_4]_n\text{-}\underline{{}^+THF} + \underline{FSO_3{}^-} \rightarrow \left.\begin{matrix}H-\\HOSO_2-\\DAS-\end{matrix}\right\}\text{-}[O(CH_2)_4]_{n+1} - \underline{OSO_2F}$$

FSO3 attack on ⁺THF *(13)*

$$\left.\begin{matrix}H-\\HOSO_2-\\DAS-\end{matrix}\right\}\text{-}[O(CH_2)_4]_n\text{-}\underline{OSO_2F} + \underline{H}\text{-}[O(CH_2)_4]_m\text{-}\left\{\begin{matrix}-{}^+THF\\-O_2SOF\\-DAS\end{matrix}\right.$$

$$\rightarrow \left.\begin{matrix}H-\\HOSO_2-\\DAS-\end{matrix}\right\}\text{-}[O(CH_2)_4]_n\text{-}\underline{DAS} + \underline{DAS}\text{-}[O(CH_2)_4]_m\text{-}\left\{\begin{matrix}-{}^+THF\\-O_2SOF\\-DAS\end{matrix}\right. + DAS$$

$$+ \underline{HF}$$

Alkyl fluorosulfate attack on OH *(14)*

$$\left.\begin{matrix}H-\\HOSO_2-\\DAS-\end{matrix}\right\}\text{-}[O(CH_2)_4]_n\text{-}\underline{{}^+THF} + \underline{HOSO_2}\text{-}[O(CH_2)_4]_m\text{-}\left\{\begin{matrix}-{}^+THF\\-O_2SOF\\-DAS\end{matrix}\right. +$$

$$\rightarrow \left.\begin{matrix}H-\\HOSO_2-\\DAS-\end{matrix}\right\}\text{-}[O(CH_2)_4]_{n+1}\text{-}\underline{DAS} + \underline{DAS}\text{-}[O(CH_2)_4]_m\text{-}\left\{\begin{matrix}-{}^+THF\\-O_2SOF\\-DAS\end{matrix}\right. + DAS$$

$$+ \underline{H^+}$$

Alkyl sulfate attack on ⁺THF *(15)*

$$HFSO_3 \rightleftarrows H^+ + FSO_3{}^- \tag{8}$$

FSA Dissociation

$$HF \rightleftarrows H^+ + F^- \tag{9}$$

HF Association

$$THF + H^+ \rightarrow H - [(CH_2)_4O]_0 - {}^{+}THF \tag{10}$$

Initiation

$$\left.\begin{matrix}H-\\HOSO_2-\\DAS-\end{matrix}\right\}\text{-}[O(CH_2)_4]_n - {}^{+}THF + THF \rightleftarrows \left.\begin{matrix}H-\\HOSO_2-\\DAS-\end{matrix}\right\}\text{-}[O(CH_2)_4]_{n+1}\text{-}{}^{+}THF \tag{11}$$

Propagation, depropagation

$$\underline{FSO_3{}^-} + \underline{H}\text{-}[O(CH_2)_4]_n\text{-}\left\{\begin{matrix}-{}^{+}THF\\-O_2SOF\\-DAS\end{matrix}\right. \rightarrow \underline{HOSO_2}\text{-}[O(CH_2)_4]_n\text{-}\left\{\begin{matrix}-{}^{+}THF\\-O_2SOF\\-DAS\end{matrix}\right. + \underline{F^-} \tag{12}$$

$FSO_3{}^-$ attack on OH

$$\left.\begin{matrix}H-\\HOSO_2-\\DAS-\end{matrix}\right\}\text{-}[O(CH_2)_4]_n\text{-}\underline{{}^{+}THF} + \underline{FSO_3{}^-} \rightarrow \left.\begin{matrix}H-\\HOSO_2-\\DAS-\end{matrix}\right\}\text{-}[O(CH_2)_4]_{n+1} - \underline{OSO_2F} \tag{13}$$

$FSO_3{}^-$ attack on ${}^{+}THF$

$$\left.\begin{matrix}H-\\HOSO_2-\\DAS-\end{matrix}\right\}\text{-}[O(CH_2)_4]_n\text{-}\underline{OSO_2F} + \underline{H}\text{-}[O(CH_2)_4]_m\text{-}\left\{\begin{matrix}-{}^{+}THF\\-O_2SOF\\-DAS\end{matrix}\right. \rightarrow \left.\begin{matrix}H-\\HOSO_2-\\DAS-\end{matrix}\right\}\text{-}[O(CH_2)_4]_n\text{-}\underline{DAS} + \underline{DAS}\text{-}[O(CH_2)_4]_m\text{-}\left\{\begin{matrix}-{}^{+}THF\\-O_2SOF\\-DAS\end{matrix}\right. + DAS + \underline{HF} \tag{14}$$

Alkyl fluorosulfate attack on OH

$$\left.\begin{matrix}H-\\HOSO_2-\\DAS-\end{matrix}\right\}\text{-}[O(CH_2)_4]_n\text{-}\underline{{}^{+}THF} + \underline{HOSO_2}\text{-}[O(CH_2)_4]_m\text{-}\left\{\begin{matrix}-{}^{+}THF\\-O_2SOF\\-DAS\end{matrix}\right. + \rightarrow \left.\begin{matrix}H-\\HOSO_2-\\DAS-\end{matrix}\right\}\text{-}[O(CH_2)_4]_{n+1}\text{-}\underline{DAS} + \underline{DAS}\text{-}[O(CH_2)_4]_m\text{-}\left\{\begin{matrix}-{}^{+}THF\\-O_2SOF\\-DAS\end{matrix}\right. + DAS + \underline{H^+} \tag{15}$$

Alkyl sulfate attack on ${}^{+}THF$

Schema (1) – Reactions used in the model. Only the reactions of equation (8) and (11) are reversible. HF does not dissociate in this system.

2.5 A Priori Conclusions about the Chemistry

From a careful study of Pruckmayr and Wu’s (1978) reactions in **equation (12)-(15),** combined with their experimental measurements, we can make a number of conclusions that support and further define the reaction system. These confirm the need to include these reactions. Since the literature doesn’t provide values for all the rate constants in the system, these will help to limit the possible values of the unknown constants.

Alkyl sulfate is present; therefore the reaction of **equation (12)** must take place. Alkyl fluorosulfate is present; therefore the reaction of **equation (13)** must take place. Alkyl fluorosulfate does not persist in the reaction system and is only destroyed by the reaction of **equation (14),** thus this reaction must take place. Alkyl sulfate is converted to dialkyl sulfate from the early hours until approaching completion at 24 hrs. The only path for this is the reaction of **equation (15)**, so this reaction must take place, and continues up until 24 hrs.

Substantial HF is created in this system, and remains as a stable end product. In water, HF, H^+, and F^- would form an equilibrium system, and high concentration of HF would lead to more dissociation to yield H^+, the chain activating agent. If this were taking place in this system, some of this H^+ would react with THF to form new active chains, thus lowering M_n over time. However, M_n appears to stabilize even in the presence of high amounts of HF. Therefore, the association of H^+, and F^- to form HF is effectively irreversible. As result, the forward dissociation rate constant of **equation (9)** is zero.

The reaction of **equation (15)** eliminates one active propagating $^+$THF center and produces H^+, which is the chain activating agent. Thus, this reaction can be considered a chain transfer to initiator. This leads to the creation of more than one chain per initiator molecule, and will result in lower M_n than produced by an ideal system.

The reaction of equation (12) produces F^-. This associates with H^+ to form HF, which remains associated in this system. Since H^+ is the species which activates monomer to form a propagating chain, F^- acts to remove the activating agent before it can activate a chain. Thus, the reaction of equation (12) will result in fewer chains being formed than the stoichiometric amount of H^+ liberated from the dissociation of $HFSO_3$. This will result in higher M_n than produced by an ideal system.

Pruckmayr and Wu (1978) used a THF/FSA molar ratio of 11.6:1. With a monomer molecular weight of 72, and monomer conversion of 61.5%, this results in an average **degree of polymerization** (**DP**) of 7.3, with M_n of 525 if each $HFSO_3$ proton activates a single chain with no chain transfer. Pruckmayr and Wu (1978) measured M_n to be substantially higher; therefore some protons never react to activate chains.

Since alkyl sulfate was measured to evolve in the first few hours and persist for 24 hours, the reaction of equation (12) must take place in the first few hours. This reaction liberates F^- which has very strong tendency to associate with H^+, irreversibly forming HF. This means the number of chains formed in the beginning hours is reduced.

The reaction of equation (15) produces H+, which forms new chains. Since this reaction continues up to 24 hrs, new chains are being formed through 24 hrs. Thus, M_n should continue to decrease through 24 hrs.

A further observation is that Pruckmayr and Wu (1978) measured M_n to be constant after 6 hrs. There are two competing effects that pertain. First, during this time, alkyl sulfate is converted to dialkyl sulfate by the reaction of equation (15). This reaction produces H^+ and thus new active chains, which acts to reduce M_n. Second, and opposite in effect, they also measured continued increasing conversion after M_n stabilized, which should act to increase Mn. The relative balance between these competing effects determines whether M_n increases, decreases, or remains constant during this time.

Pruckmayr and Wu's (1978) experiments show that all of this chemistry takes place in the polymerizing mixture. However, we don't know how important these secondary reactions are to the properties of the resulting oligomer. Simulation can give us this insight.

3 Scope of this Model

In their recent comprehensive review of industrial polymerization modeling, Mueller, Richards and Congalidis (2011) lay out the four centers of focus in such models: reaction kinetics, phase equilibrium thermodynamics, mass transfer, and particle dynamics. However this system is considerably simpler. The monomer conversion is limited by the reversibility of the propagation, and the degree of polymerization is relatively low. Thus, the polymerizing system remains a liquid system, with oligomer dissolved in monomer. There are no particles formed, eliminating particle dynamics. The reacting liquid is below the boiling point of the monomer, and so there is no significant second phase, eliminating phase equilibrium. The reacting mass remains a moderately viscous fluid, so there are no cage or gel effects, eliminating mass transfer. Thus, the system can be adequately described with reaction kinetics alone.

This study treats the system as isothermal. The reacting mass of this system can be stirred, so good temperature control can be achieved in a commercial reactor using vessel cooling. An isothermal assumption gives a model that is industrially useful, and is used here.

The temporal measurements of conversion, M_n, sulfate and fluorosulfate concentrations were made by Pruckmayr and Wu (1978) at 25ºC. These measurements and this temperature are the basis for evaluating the ability of a model to reproduce this chemistry.

4 Simulation Development

4.1 Rate Constants and Initial Conditions

To model this system, kinetic rate constants and concentrations are needed. Some reactions have published rate constants. Kobayashi, Danda, and Saegusa (1973) published initiation and propagation rate constants at three temperatures for THF polymerization initiated with the ethyl ester of fluorosulfate: $Et\text{-}OSO_2F$. These values allow the constants to be calculated at any nearby temperature. Their values of the initiation rate constant: k_i (8.4 ºC) = $0.67\text{x}10^{-5}$

$l\cdot mol^{-1}\cdot sec^{-1}$ and k_i (0 °C) = $0.33x10^{-5}$ $l\cdot mol^{-1}\cdot sec^{-1}$ can be used to derive the temperature dependent expression:

$$k_i\ (T)\ =\ 6.63\ x10^4 \exp\left(\frac{-12824}{R\ T}\right) \qquad (16)$$

where R=1.98 $cal\cdot mol^{-1}\cdot\ {}^oK^{-1}$ and T is in ºK. Similarly, their values of k_p (0 ºC) = $0.66x10^{-3}$ $l\cdot mol^{-1}\cdot sec^{-1}$ and k_p (8.4 ºC) = $1.4x10^{-3}$ $l\cdot mol^{-1}\cdot sec^{-1}$ give the temperature dependent expression:

$$k_p\ (T)\ =\ 5.75\ x10^7 \exp\left(\frac{-13617}{R\ T}\right) \qquad (17)$$

Saegusa (1972) derived the equilibrium relationship between the forward and reverse rate constants for propagation:

$$k_{-p} = k_p \cdot [THF]_e \qquad (18)$$

where $[THF]_e$ is the concentration of THF when the propagation and depropagation reactions are at equilibrium. Pruckmayr and Wu (1978) give a final conversion of THF of 61.5% in 15.5 mol% $CDCl_3$, a non-polar solvent similar to that used in their measurements of F and S containing groups. This can be taken as the equilibrium value. Then, assuming ideal mixing, using published densities, and assuming no volume change with polymerization, this conversion gives $[THF]_e$ =(1.0-0.615) · 9.57 mol · l^{-1} = 3.68 mol · l^{-1}, thus

$$k_p(25\ °C) =\ 0.0055\ \ l\cdot mol^{-1}\cdot sec^{-1} = 19.8\ \ \ l\cdot mol^{-1}\cdot hr^{-1} \qquad (19)$$

$$k_{-p} = k_p \cdot [THF]_e = 0.0202\ \ sec^{-1} = 72.8\ \ hr^{-1} \qquad (20)$$

$$k_i(25\ °C) =\ 2.41x10^{-5}\ \ l\cdot mol^{-1}\cdot sec^{-1} = .0868\ \ \ l\cdot mol^{-1}\cdot hr^{-1} \qquad (21)$$

Kobayashi, Danda, and Saegusa (1973) used a superacid ester as initiator, while Pruckmayr and Wu (1978) used the superacid. The ester initiation reaction results in an oxonium ion whose “chain tail” is an ethyl group, while the acid initiation forms an oxonium ion with a hydrogen atom at that location. Although strictly the steric chemistry is different, both create an oxonium ion site for attack by THF. There are no published results that would let us distinguish the rates of these two initiations, and given the similarity, it is a reasonable assumption to take the rate constant for the ester form as a good approximation to the rate constant in the superacid system.

Assuming ideal mixing, using published specific gravity, and dropping the $CDCl_3$ from Pruckmayr and Wu's (1978) initial molar ratio of 11.58/2.31/1.00 mol THF/ $CDCl_3$/$HFSO_3$ gives an initial molar ratio of 11.58/1.00, and initial concentrations of $[THF]_0 = 11.6\ mol \cdot l^{-1}$ and $[HFSO_3]_0 = 1.00\ mol \cdot l^{-1}$.

For the remaining rate constants, there are no published values. To create a model, it's possible to explore values by trial and error, comparing the time profiles of F-containing groups to Pruckmayr and Wu's (1978) Table II and comparing the time profiles of S-containing groups to Pruckmayr and Wu's (1978) Table IV. There is a single reaction path leading to/from three important groups: FSO_3^-, alkyl sulfate (AS), and fluorosulfate (AFS):

$$\begin{array}{l} \mathrm{HFSO_3} \rightarrow \mathrm{FSO_3^-} \rightarrow \mathrm{AFS} \\ {}^{+}\mathrm{THF} + \mathrm{FSO_3^-} \rightarrow \mathrm{AFS} \rightarrow \mathrm{DAS} \\ \mathrm{HO\text{-}X} + \mathrm{FSO_3^-} \rightarrow \mathrm{AS} \rightarrow \mathrm{DAS} \end{array} \qquad (22)$$

Since we know the time profiles of these groups, and there is no competition between different reactions creating/consuming these species, it should be possible to use trial and error to find rate constant values, and it seems likely the values found this way will be unique.

4.2 Lumped Simulation Development

Although chemical kinetics are usually approached by making a balance on each type of molecule in the system, for polymer systems the large number of differing polymer compounds (of varying chain lengths) make such an approach difficult. A lumped approach, making the balance around a polymer species including all chain lengths of that species, does not provide as much detail as a full distributed model, but it may be much easier to solve. This approach was used first in this study.

4.2.1 Computation Method

A lumped model treats all chains having the same end groups as a single component. For example, both $H\text{-}[O(CH_2)_4]_2\text{-}\,{}^{+}THF$and $H\text{-}[O(CH_2)_4]_8\text{-}\,{}^{+}THF$, having chain lengths of 2 and 8 monomer units but sharing common end groups, are lumped or counted together as $H\text{-}[O(CH_2)_4]_n\text{-}\,{}^{+}THF$. The propogation reaction of equation (11) makes no change in this concentration; only in the concentration of THF.

Pruckmayr and Wu (1978) ran batch experiments, so it is straightforward to develop the batch reactor model balances needed to reproduce their results. Because of the multiplicative combinations of end groups, the balances include many terms, which can be illustrated by the model balance for F^-, which is one of the simplest. F^- participates in the reactions of equation (9) and (12). Where square brackets denote concentration in mol·l^{-1}, $(O(CH_2)_4)_m$ means any value for m, and $k_{n,forw}$ is the forward rate constant for the reaction of equation (n), its balance is:

$$\frac{d[F^-]}{dt} = k_{9,forw} \cdot [HF] - k_{9,rev} \cdot [H^+] \cdot [F^-] + k_{12,forw}\,[FSO_3{}^-] \cdot \{[H\text{-}(O(CH_2)_4)_m\text{-}\,{}^{+}THF] + [H\text{-}(O(CH_2)_4)_m\text{-}O_2SOF] + [H\text{-}(O(CH_2)_4)_m\text{-}DAS]\} \qquad (23)$$

This example shows the three chain families having OH end groups, all of which react with FSO_3^- to change the F^- concentration. For the reactions of equation (14) and (15), the complexity goes up by the square of the variants, and the balances for the components involved in those reactions require even more terms. While simple enough in principle, there are nine possible 9 possible combinations of reacting components for the reactions of equations (14) and (15), each involving summed terms for each of the 8 components involved. Properly closing the balances on F-containing and S-containing components requires meticulous care in writing these complex rate expressions.

The reactions of equation (8) through (15) involve 16 components, including the pseudo-component DAS, and the dynamic balances on these form a coupled system of ordinary differential equations (**ODE**'s) - one ODE for the change in concentration of each component with time. Such a system is easily solved using a numerical integration package. The reactions present in this system are diverse, and the experimental data shows fast changes in M_n while other components, such as those containing alkyl sulfate, are changing slowly. Thus, stiffness seemed likely and suggested the use of a stiff ODE algorithm. For this study, the balances were coded in FORTRAN and the system solved with the DDRIV2 solver using the stiff-capable, implicit Gear method. (Later, the Gear method proved intractable for the distributed model because of the large n^2 matrix required for that method, and it then became clear that the distributed system is non-stiff and solves adequately using the explicit Adams solver. Thus, it's likely the lumped model is not stiff, although this was not tested.)

4.2.2 Limitations of the Lumped Approach

Lumping related compounds reduces the scope of the problem significantly. However there are three errors introduced by this simplification, and later we'll see that these significantly impair the ability of the resulting model to reproduce the conversion dynamics of this system.

First, the chemistry, as defined, does not include the reverse initiation reaction. Once a proton attacks a THF molecule to form the secondary oxonium ion, the decomposition to return a proton and a THF molecule is assumed to be so slow that it can be ignored. However, this activated monomer falls within the lump for active polymerizing chains, and all species within this lump reverse propagate. To calculate the reverse propagation (depropagation) reaction, the only value available in the lumped model is the lumped concentration, which includes the activated monomer. So, when computing the change in THF concentration, the contribution from reverse propagation includes the reverse initiation. Reverse initiation is a reaction that is not believed to take place, and so was specifically excluded from the reactions to be modeled.

If the system were making a high polymer, this might be negligible. This isn't true for an oligomer like PTMEG, and as is shown later by the distributed model, the concentration (or number fraction) of chains is largest for chain lengths of one, so the error involves the one component of this family with the most effect. Moreover, because of the lumping, this reverse initiation is calculated using the reverse propagation rate constant and not a reverse initiation rate constant defined by the chemistry. The chemistry of decomposition of an oxonium ion to re-form THF monomer should be substantially different from the depropagation reaction and, assuming this reaction proceeds at all, the imposed use of the wrong rate constant would further add to the error in the lumped model.

Second, the balances for H^+ and the propagating chains are not consistent with the THF balance. The THF balance, as just described, must include the reverse initiation reaction. To be consistent, the H^+ balance needs to include the H^+ produced from this reverse reaction, and the active chain balance must account for the loss of an active chain. However, these contributions can only be calculated using the n=0 chain length concentration (the activated monomer concentration) and this is not known in the lumped formulation. Ideally, if every H^+ formed by this reaction would result in a new chain, these two errors exactly offset one another in their impact on the number of active chains, which means together they wouldn't impact M_n. However, we know that F^- reacts with H^+, removing some of the resulting chain initiating capacity, so here again there is some error introduced.

Third, there are two families of propagating species whose non-polymerizing ends terminate in HO_3SO- and in FO_2SO-. It seems chemically improbable that the n=0 chain length members of these two groups could decompose at all, since instead of yielding H^+ , they would have to produce highly unlikely positively charged sulfate and fluorosulfate ion groups. But because the n=0 species are lumped with the higher chain lengths, which must reverse propagate, these chemically unlikely reactions are included the model balances.

Conceptually, these limitations are troubling. It is not that approximations are made which reduce the accuracy of the lumped model solution. Rather, these limitations mean that the lumped formulation is modeling a different kinetic system than was defined by the chemistry. But the lumped model may still have value. For example, process development or optimization might require integrating the reactor model into a dynamic flowsheet simulator. A lumped model could probably be integrated with reasonable effort. However, the size and complexity of a full distributed model probably make this integration impossible. So, it is worthwhile to make the lumped simulation and compare it later to the full distributed model to see how significant these limitations are. If the prediction errors are not too great, the lumped model may have significant value.

4.3 Distributed Simulation Development

4.3.1 Balances for the Distributed Model

In a lumped model, the complexity of the model is reduced by making balances around families of species with the same end groups, including species of all chain lengths. For a distributed model, each different chain length within a family has its own balance. In some cases, the balance for an individual species, like F^-, will become more complex because F^- is a product of the reaction of equation (12), and so there will be contributions to the rate of creation of F^- in its balance which involve chains of the form $H\text{-}[O(CH_2)]_n\text{-}^{+}THF$ for all values of n.

The three propagating species in the reactions of equation (11) require special care in their balances for the contributions from initiation, propagation, and depropagation. Initiation only contributes to the formation of the OH terminated compound of chain length 0. As stated above, the initiation reaction in this system is taken to be irreversible, and therefore none of the three propagating species of chain length 0 can depropagate (literally, decompose) to liberate THF. In principle, if we wanted to consider this reaction, it would best be treated using a unique reverse initiation rate constant ($k_{10,rev}$)and not the reverse propagation constant ($k_{11,rev}$, as the lumped model structure requires), because the reverse initiation reaction is chemically different from the reverse propagation reaction.

Also, for any discrete polymerization model, a maximum length must be chosen and balances made around chains of each length up to this limit. This requires the approximation that propagating species of the maximum length cannot further propagate. If this limit is set too low, concentration of polymer at the highest chains lengths will accumulate, resulting in an elevated tail on the distribution.

In the lumped model, there were balances for nine chain species: the three chain ends that can result from the initial OH end group combined with the three chain ends that can result from the activated $^{+}$THF end group. In the distributed model, it is necessary to make balances around each chain length within each of these nine families of chains. So if, as chosen here, it is necessary to track chains up to a DP of 100, then 900 balances on chain species are needed, plus the balances on the simple species such as HF.

4.3.2 Computational Method

The distributed model was solved by the same approach as the lumped model. Balances were coded in FORTRAN as coupled ODEs, and solved numerically using the DDRIV2 solver. The system solved adequately using a non-stiff, explicit Adams method.

4.3.3 Ring Opening and Chain Length

In the lumped model, no account is taken of changes in chain length, only the creation or destruction of a particular kind of chain. The distributed model requires accounting for formation/destruction of chains of each length. Changes in chain length happen by three mechanisms. First, length changes by propagation/depropagation of equation (11). Second, the reactions of equation (13) and (15) open the ring of the $^{+}$THF end group, forming another monomer segment to the chain. And last, the water extraction which is the customary downstream processing of the polymerization mixture will also open all remaining $^{+}$THF rings to form a monomer segment.

For final product properties, it makes no difference when the ring opening of equation (13) and (15) is accounted for. There are two classes of chain ends on the +THF end: those that remain active as +THF and those that have been ring-opened by the reactions equations (13) and (15). Both forms will ultimately be opened. It is equally effective to account for the ring opening at the time of the reaction, or to simply account for both methods of ring opening at the end when the water extraction is assumed to be complete. Since it is quite a bit simpler to save the change caused by the reactions of equation (13) and (15) until the end, this method was used. So, using this convention, what has been called the n=0 form (the activated monomer with no additional monomer segments) becomes n=1 (monomer) after water extraction. Unlike all the longer chains, it remains in ring form (as THF) and does not form a linear diol, but this does not impact the MWD.

5 Simulation Results and Discussion

5.1 Lumped Simulation Results

5.1.1 Heuristic Fit Lumped Rate Constants

Using the rate constants calculated from literature values and the conclusions described above, a lumped simulation was developed. Initial guesses were made for the unknown rate constants. Based on the simulation results, these were adjusted to move the results closer to the experimentally observed behavior. Much of the observed behavior can be reproduced, but Pruckmayr and Wu’s (1978) simultaneous measurement of stable M_n after 6 hrs cannot be reconciled with the still changing alkyl sulfate concentration. Using one set of rate constants, the proper magnitude and timing of the relative alkyl sulfate/dialkyl sulfate concentrations can be achieved, but M_n does not stabilize until about 20 hrs (Run 86). Using a different set, M_n stabilizes around 6 hrs, but the shift from alkyl sulfate to dialkyl sulfate occurs much earlier and is mostly complete by 6 hrs (Run 89). There are several factors that might be considered when trying to explain these discrepancies, but as shown later with the results of the distributed model, the inaccuracies in the lumped representation of the kinetics (discussed above) are the reason for these mismatches.

It seems most reasonable to assume that M_n continues to change with time, because this fits the multiple alkyl sulfate measurements, seems consistent with the changing conversion, and accords with the overall chemistry. Accepting this, the rate constants that give the chosen best fit (Run 86) are given in **table (1)** indicated by either "both" or "lump" under "Model".

5.1.2 Results: Comparison to Experiments

The simulation result is shown in figure (1) through figure (3), in combination with the Pruckmayr and Wu (1978) measurements as given in their Table II, Table IV, and Table VI. Pruckmayr and Wu (1978) did not report continuous measurements, so the dashed lines through the Pruckmayr and Wu (1978) data points are interpolated. The model results are shown by a solid line.

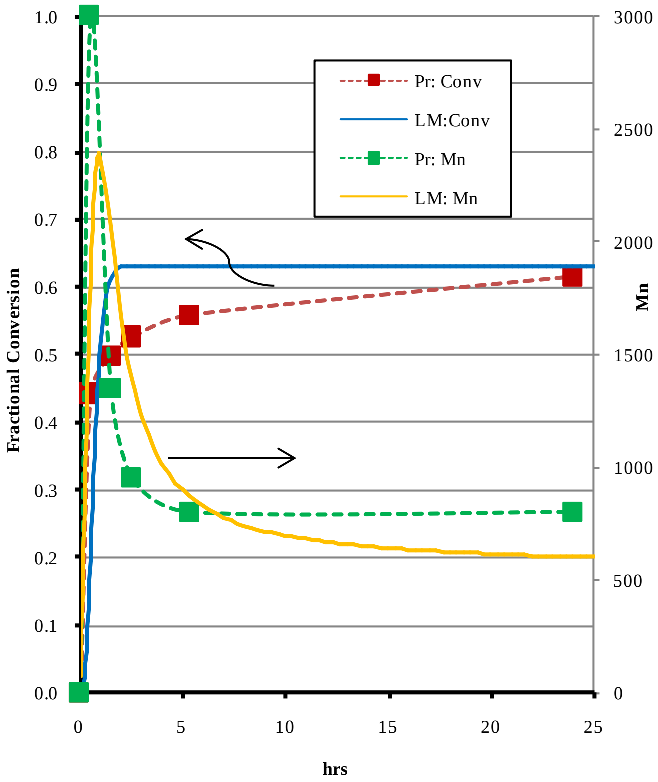

Figure (1) – Lumped Model (LM) Simulation: Number average molecular weight (M_n) and THF Conversion (Run 86) compared to measurements of Pruckmayr and Wu (1978) (Pr) in 15.5 mol% $CDCl_3$ (non-polar.) Rate constants from table (1) indicated by either "both" or "lump". Dashed lines are interpolated.

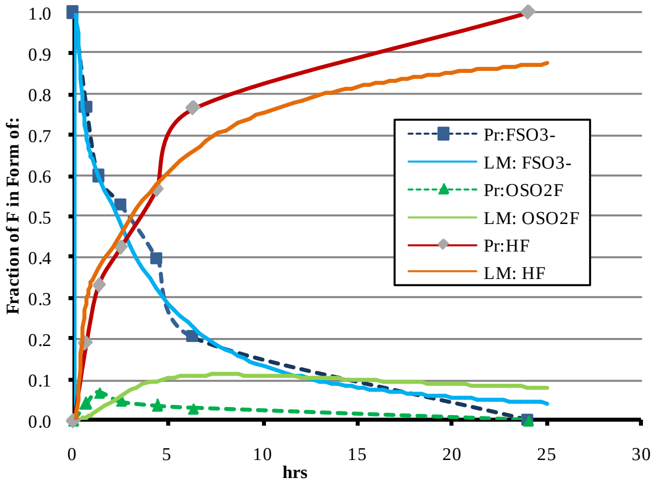

Figure (2) – Lumped Model (LM) Simulation: Fraction of Fluorine in 3 forms (Run 86); compared to F-NMR measurements of Pruckmayr and Wu (1978) (Pr) in 20 mol% CH_2Cl_2 (non-polar.) OSO_2F is alkyl fluorosulfate. Rate constants from table (1) indicated by either "both" or "lump". Dashed lines interpolated. Distributed model results are effectively equivalent.

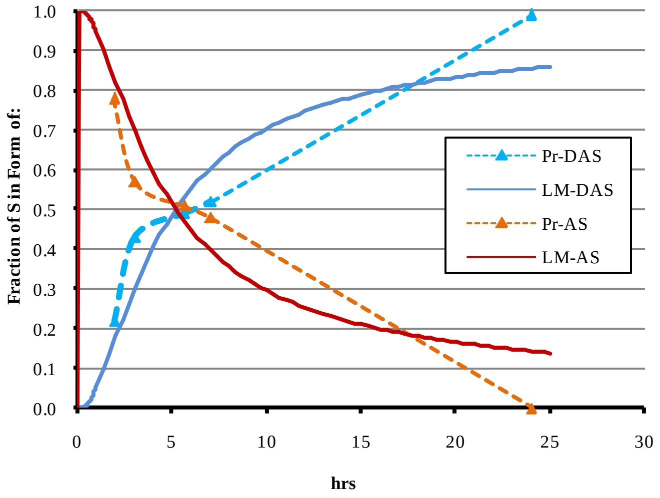

Figure (3) – Lumped Model (LM) Simulation: Fraction of sulfur in 2 forms: alkyl sulfate (AS) and dialkyl sulfate (DAS); compared to H-NMR measurements of Pruckmayr and Wu (1978) (Pr) in 15.5 mol% $CDCl_3$ (non-polar.) Rate constants from table (1) indicated by either "both" or "lump". Dashed lines interpolated. Distributed model results are effectively equivalent.

5.1.3 Propagation Rate Constants and the n=0 reverse propagation

Table (1) shows that the best fit found with the lumped model uses the exact forward rate constant computed from Kobayashi, Danda, and Saegusa (1973), and only a modest adjustment to their reverse rate constant. As shown later by the distributed model results, these constants are far too small to reproduce the experimental results when used with the correct kinetics in the distributed model. Yet they perform well in this lumped formulation.

The agreement can be explained directly. Kobayashi, Danda, and Saegusa (1973) based their data analysis on the kinetic derivation of Saegusa (1972). Saegusa's equation (2) writes the monomer balance using a lumped formulation: both forward and reverse rates of reaction depend on the sum of all active polymerizing chains. This is equivalent to the lumped formulation used here, and it also includes the reverse polymerization to monomer. Thus, the Kobayashi, Danda, and Saegusa (1973) rate constants result from a fit of experimental data to a kinetic model that exactly matches the lumped formulation used here, and it's not surprising that their rate constants work in this formulation.

5.1.4 FSO_3^- Reactions and Molecular Weight Distribution

As for any polymer, the properties of polymerized THF strongly depend on the molecular weight distribution (MWD) that is created. Since MWD is not easily measured, any approach that can give a MWD for a polymer without that measurement is quite valuable. Obviously, this study is focused on the use of dynamic kinetic simulation to model MWD, but in assessing the value of the substantial effort to simulate a system like this, it is important to consider other approaches that might more easily give a MWD or an estimate of the MWD.

Before computers existed, analytical approaches yielded shapes and/or values of MWD. For stepwise polymerizations, Flory (1936) showed by statistical arguments that the MWD follows the Flory distribution as a function of the **extent of reaction *p*** (the fractional conversion of monomer to polymer), where f_n **(the fraction of polymer molecules having number chain length n)** is given by

$$f_n = p^{n-1}(1-p) \qquad \text{Flory Distribution (17)}$$

Unfortunately, this important relationship does not apply to the system studied here for two reasons. First, this system is a chain polymerization, in which (ideally) the number of propagating sites is equal to the starting number of initiator molecules. Flory (1936) based his derivation on the assumption that every monomer and chain end has equal probability of reacting, which does not apply to this system. Second, this system is reversible, which adds complexity to the analysis, while Flory's (1936) analysis assumed irreversible formation. Clearly, given the equilibrium monomer conversion around 0.6 measured by Pruckmayr and Wu (1978), the Flory (1936) expression for the chain fractions would decrease very quickly with increasing chain length, giving a very low MWD, which is not the case.

Brown and Szwarc (1958) studied living, reversible polymerizations in chain growth systems - essential qualities much closer to this system. They considered systems without any initiation reaction (thus activated monomer is present initially); without termination or chain transfer; and where the active dimer cannot depropagate to recreate the activated monomer. Because of the reversibility of propagation, and because the active polymerizing centers remain able to polymerize and depolymerize, all such "living" systems will reach an equilibrium steady state. They showed that f_n at equilibrium is given by

$$f_n = f_1(1 - f_1)^{n-1}$$ Brown and Szwarc (1958) Distribution (18)

This distribution shares fundamental shape with the Flory (1936) expression for stepwise polymerizations. Unlike the Flory (1936) expression which directly gives the quantitative distribution if one knows the monomer conversion, Brown and Szwarc (1958) requires knowing f_1, and it isn't clear how this could be measured.

The Brown and Szwarc (1958) requirement that activated monomer is present at the outset need not be a barrier to applying their formula to this system. Their analysis is based on a steady state assumption, which means it applies at long reaction times. At long times, the initiation reaction will proceed to completion, thus giving the same concentration of active chains that Brown and Szwarc (1958) assume. However, this system includes the termination reactions of equation (13) and (15), and the chain transfer reaction of equation (15). The Brown and Szwarc (1958) analysis can only be applied if these differences can be shown to be insignificant, which is explored below.

5.1.5 FSO_3^- Reactions Make Brown and Szwarc (1958) not Accurate

In the absence of the reactions involving the counter ion FSO_3^-, the chemistry of this system would almost match the restrictions needed for Brown and Szwarc (1958), and such a system might produce a MWD according to their formula of **equation (18)**. (However, their requirement that active dimer not depropagate to active monomer conflicts with the chemistry defined here, and this could still be significant.) But here, we need to know if the FSO_3^- termination reactions of equation (13) and (15) can be neglected before we can determine whether equation (18) applies. We know already that M_n goes through a significant spike early in the batch reaction. If these termination reactions proceed at a significant rate during the spike when long chains exist, then long chains will be terminated and the MWD will be shifted higher, away from the Brown and Szwarc (1958) distribution. If this effect is significant, the MWD will not be properly represented by the Brown and Szwarc (1958) formula.

To explore this, we can create three additional pseudo components in the lumped simulation. The first results from integrating the forward rate of the reaction of equation (13) and shows the cumulative concentration of active chains that are terminated by reaction with FSO_3^-. The second results from integrating the forward rate of the reaction of equation (15) and shows the cumulative concentration of active chains that are terminated by reaction with alkyl sulfate. The third results from integrating the forward rate of monomer initiation, which gives the cumulative concentration of active chains formed (even if subsequently terminated.)

Figure (4) shows these results during the early part of the reaction. The two lowest trend lines are the integrated concentration of chains terminated by FSO_3^- and alkyl sulfate reactions. At t=1.66 hr, after most of the M_n peak has passed, 0.062 mol·l-1 of chains have been terminated by FSO_3^- reactions, out of a total of 0.27 mol·l-1 of chains activated. Thus, 23% of the chains in the reaction mixture at that time were terminated during the M_n peak. By the 6 hr time at which Pruckmayr and Wu's (1978) measurements showed that M_n had stabilized, 0.64 mol·l-1 of chains have been activated, thus 10% of the chains present at 6 hrs had their length fixed during the M_n peak, when M_n was about four times the final value.

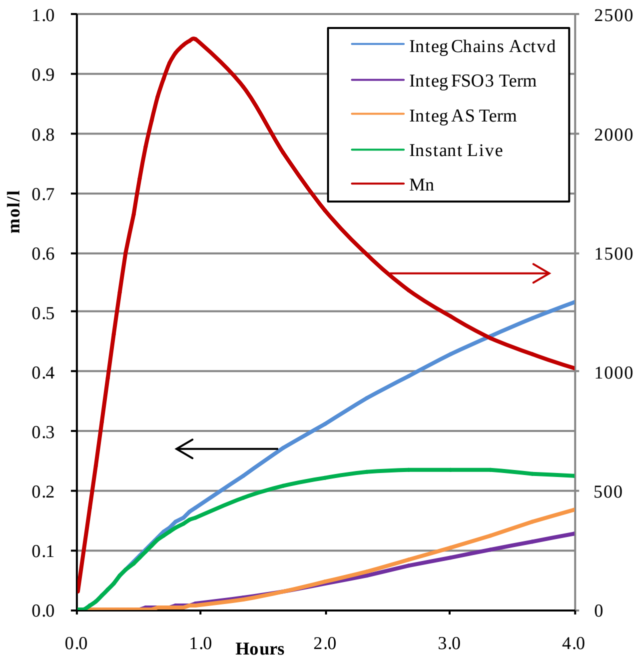

Figure (4) – Lumped Model (LM) Simulation (Run 99) showing the integral concentration of chains activated, terminated by FSO_3^-, terminated by alkyl sulfate (AS); and the instantaneous number of active chains (Live) mol·l^{-1}; and the number average molecular weight (M_n - right hand scale).

This analysis shows that the FSO_3^- and alkyl sulfate termination reactions must have a significant effect on the MWD of this system. So, the MWD will differ from that predicted by the Brown and Szwarc (1958) formula and this difference could significantly change the resulting PTMEG properties. It also means that any simulation intended to predict the MWD of this system needs to include these reactions and, by necessity, also the reactions that give rise to alkyl sulfate.

There is another way to evaluate the effect of the FSO_3^- reactions on M_n. Because this reversible polymerization has monomer conversion set by the ratio of the forward and reverse propagation constants, the final M_n is only dependent on the number of chains formed and isn't affected by the termination of chains during the M_n spike. But, the reaction of equation (12) creates F^-, which reacts quickly with H^+ to irreversibly form HF, eliminating activator H^+ before it can form a chain. So the FSO_3^- reactions reduce the number of chains that can be activated, and the resulting M_n will be higher than without these reactions.

This can be evaluated by setting the rate constants of the reactions in equations (12) through (15) to zero. The result is a final M_n of 525 (Run 100.) M_n is 600 when the reactions are included, again showing a significant effect of the FSO_3^- reactions on average molecular weight.

5.2 Distributed Simulation Results

5.2.1 Results: using Rate Constants from the Lumped fit

As noted above, the lumped model formulation cannot completely represent the kinetics as they have been defined. It forces depropagation to be included for chains of length 0, it neglects the contribution to H^+ from this reaction, and it fails to account for nonsense F and S containing ions that must be created.

The distributed model, which correctly addresses these issues, is compared to the lumped model, both models using the rate constants found for the lumped model. Figure (5) shows the results for maximum DP of 100. It's immediately obvious that the shape of the conversion vs. time curve in the distributed model is nearly identical to the experiments, while the lumped model deviates from experiments. Also, using the same rate constants, the lumped model produces a much lower conversion than the distributed model. The difference results from depropagation to monomer in the lumped model, which is properly absent in the distributed model. As shown later in the MWD results, the n=1 chains have the highest concentration of all chains lengths, and so properly excluding this reaction is quite significant.

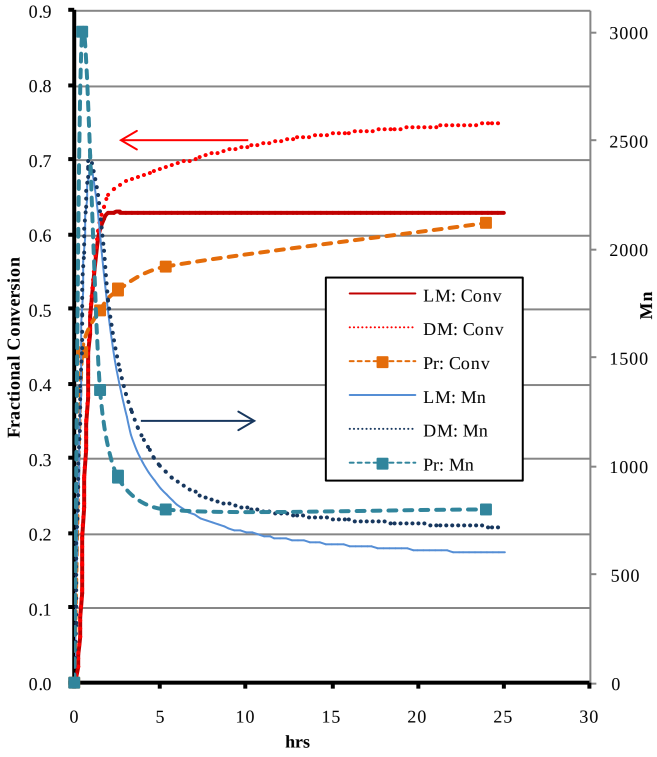

Figure (5) – Lumped model (LM) results (Run 86) and distributed model (DM) results (Run 150) for THF Conversion and M_n compared to measurements of Pruckmayr and Wu (1978)

(Pr) in 15.5 mol% $CDCl_3$ (non-polar.) Rate constants in both models are best lumped values from table (1) indicated by either "both" or "lump". Dashed lines interpolated.

5.2.2 Heuristic Fit Distributed Rate Constants

It is striking that correctly eliminating the n=0 depropagation terms in the distributed model makes the conversion profile take virtually the same shape as the experiments. However, using the best rate constants from the lumped model, conversion in the distributed model is significantly higher than the lumped model and the measurements. Thus, the rate constant search must be resumed to seek a better match. This isn't surprising, since Saegusa (1972) used the lumped model kinetic formulation in fitting the experimental data to derive his rate constants.

Using again a manual, heuristic search, rate constants were found to best match the experimental data. These are given in **table (1)**, indicated as "both" or "distrib".

5.2.3 Results: Comparison to Experiments and Lumped Model

The simulation results, showing the values that are also available from the lumped model and the Pruckmayr and Wu (1978) experiments, are shown in **figure (6).** The results for fraction of F and fraction of S are not shown because they are nearly identical to the lumped simulation. The very small difference is likely the result of summing individual concentrations and reaction rates vs. using lumped values.

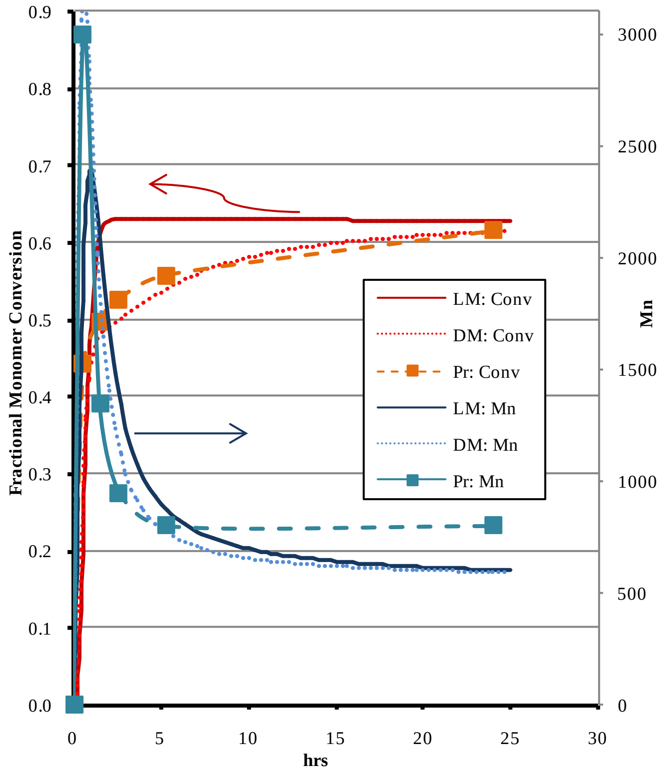

Figure (6) – Lumped model results (LM) (Run 86) and distributed model results (DM) (Run 149) for THF Conversion and M_n compared to measurements of Pruckmayr and Wu (1978) (Pr) in 15.5 mol% $CDCl_3$ (non-polar.) Each model uses its own best fit rate constants from table (1); lumped indicated by "lump" and distributed indicated by "distrib". Dashed lines interpolated.

The conversion profile of the distributed model is very close to Pruckmayr and Wu's (1978) measurements. By adjusting the forward and reverse propagation rate constants of Kobayashi, Danda, and Saegusa (1973) upward by 3x and 5x, the spike in M_n can be matched closely, and the initial transition from the spike in M_n into the final value matches fairly well. However, just as in the lumped model, M_n continues to drop in the final hours of the reaction as monomer conversion continues to increase.

The two simulations (LM and DM) shown in figure (6) illustrate the strong impact on model results from correcting the n=0 reverse propagation error. The conversion profile changes from a hockey stick to the more natural curve of the experiments. The profile in M_n can be matched rather closely. The forward and reverse propagation constants take values up to 5 times larger than those derived when the n=0 reverse propagation is used. These results support the choice of the kinetic scheme; that monomer is not liberated by the reverse of the initiation reaction. Chemically, this is sensible. The initiator (H^+) is a high energy entity, and it reacts with monomer, forming a lower energy product. The reverse reaction requires an energy input; which is absent in this system. Thus, we should expect initiation to be effectively irreversible, and a kinetic formulation that expresses this should better fit the experiments, as we see.

Another reason the rate constants differ is the assumption of steady state in the derivation by Saegusa (1972) in equation (18). However, in this system there are chain transfer and termination reactions, and the conversion is not at steady state but continues to change.

5.2.4 Decreasing M_n at longer reaction times

As mentioned above, the balance of [1] H^+ created from the reaction of equation (15) producing new chains (thus lowering M_n) vs. [2] the increase in conversion (thus increasing M_n) will determine how M_n changes later in the reaction. **Figure (7)** shows these two quantities. M_n at 6 hrs is 737, or 10.2 monomer units per chain. Figure (7) is scaled 10.2:1 so that for M_n to stay constant after 6 hours, the two lines must trend equally on the plot. The total chain concentration trend line increases more than the THF trend line, and so M_n must go down.

Other measurements of Pruckmayr and Wu (1978) accord with this. Significant changes are still taking place past 6 hours in their measurements for conversion shown in figure (6), for fluorine-containing species in figure (2), and for sulfur-containing species in figure (3) (distributed model results for these are equivalent to the lumped model as shown in those figures.) Most important, the continuing conversion of alkyl sulfate to dialkyl sulfate can only occur by the reaction of equation (15), leading to H^+ and thus to new chains. Taken together, these measurements and model results lend support to the continued decrease in M_n during this time, contrary to the single measurement at 24 hours of Pruckmayr and Wu (1978).

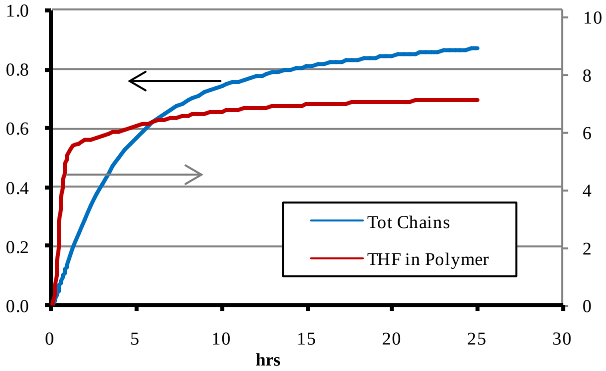

Figure (7) – Distributed model result (Run 149) for total concentration of polymer chains and equivalent concentration of monomer already reacted to form polymer; mol·l-1 . Rate constants from table (1) indicated by either "both" or "distrib".

5.2.5 MWD with Best Fit Rate Constants

Of course the distributed model not only allows the kinetics to be precisely expressed, it produces the full molecular weight distribution. Since the focus here is to reproduce the experimental results of Pruckmayr and Wu (1978), the MWD resulting from this simulation is not for any of the commercial PTMEG formulations, but is determined by the conditions used by Pruckmayr and Wu (1978): batch reactor; 11.6:1.0 monomer:initiator ratio; 25 ºC.

The number molecular weight distribution at times over the course of the reaction is shown early in the reaction in **Figure (8)** and later in the reaction in **Figure (9).** As discussed above, the customary downstream water extraction used in process plants hydrolyzes all end groups and all disulfate linkages, converting them to OH. Thus, all chains of the same length regardless of end groups are summed to get the equivalent MWD for a process plant.

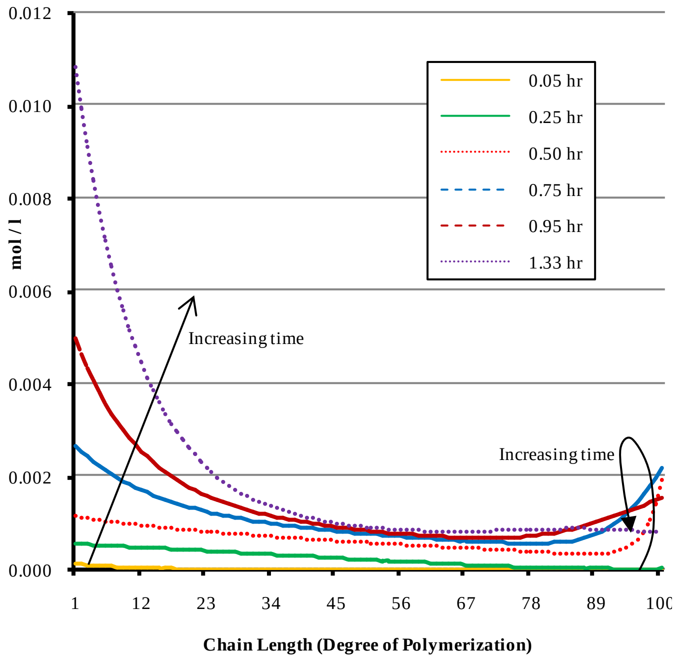

Figure (8) – Molecular weight distribution (MWD) summing all chains with same DP regardless of end groups (Run 149) early in the reaction; mol·l^{-1} . The elevated tails arise briefly when chains longer than 100 have significant concentration. Rate constants from table (1) indicated by either "both" or "distrib"; max DP:100.

At very short reaction times, THF concentration is still high. This accelerates the forward propagation, and the distribution of chain lengths is nearly flat. By 0.5 hour, the drive toward very long chains produces an elevated tail at the maximum DP of 100 and the few preceding lengths. This means that longer chains should be forming, but since the model does not allow propagation higher from the maximum DP, the chain growth toward higher DP accumulates, causing the tail. The highest value reached by the tail is 0.0024 mol . l-1 at 0.65 hour, compared the highest single DP concentration of 0.158 for n=1 at 25 hours, or 1.5% of the largest comparable concentration. The tail is short-lived and falls back by 1.33 hour. The propagation is reversible, and so, once the tail has receded, it has no further impact on the kinetics or the resulting distribution. If the tail was larger or persisted long, increasing the maximum DP of the model might improve the result.

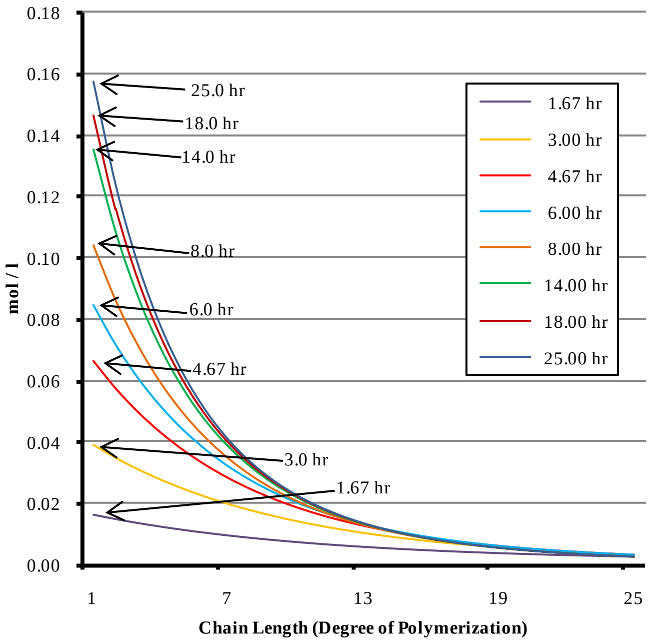

Figure (9) – Lower range of the molecular weight distribution (MWD) summing all chains regardless of end groups (Run 149) later in the reaction; mol·l^{-1} . The concentration axis scale is 15 times that of Figure (8). Rate constants from table (1) indicated by either "both" or "distrib"; max DP:100.

At longer times, the distribution grows mainly by adding shorter chains. The difference is that at longer times, the monomer concentration is lower, and the forward propagation reaction slows while the reverse is not affected. As figure (4) shows, only a fraction of the chains are alive and able to propagate, but those that are alive will tend to shorten during this time. The dead chains can’t change, and their impact on the distribution is more evident when we look at the weight fraction distribution below.

The number average molecular weight, the weight average molecular weight (M_w), and the polydispersity index (Mw/Mn) are shown over time in Figure (10). Manufacturers don't appear to publish any MWD information nor the polydispersity of their products. Balster, et al. (2011) state that the polydispersity index of commercial PTMEG is usually 2.0 ± 0.2. Before the water extraction downstream of the polymerization, Pruckmayr et al. (2000) report that 2.0 is the "theoretical" value, and that the water extraction partially removes the short chains and reduces the index to 1.6 or less.

It appears, from the trends in Figure (10), that M_w is strongly influenced by the long chains that are terminated early by the FSO_3^- reactions. M_n, indifferent to chain length, is more affected later in the reaction as more new chains are formed, because the number weighting in that index gives equal weight to those short chains. Thus, the termination of chains by FSO_3^- reactions raises the polydispersity index of the polymerization product above the "theoretical" value of 2.0.

The MWD results shown in Figure (8) through (13) are for the polymerization reactor contents after hydrolysis. As described above, the reactor product is normally extracted with water. This not only hydrolyzes the end groups to produce OH ends, it removes part of the very short chains: DP of 2 through 4. Since these have the highest number fractions, removing them in the extraction will strongly influence the number average molecular weight and also impact the weight average molecular weight, though somewhat less. However, the process effects of removing some of the shorter chains are beyond the scope of this study. Here the hydrolysis is assumed complete but no removal of short chains is considered.

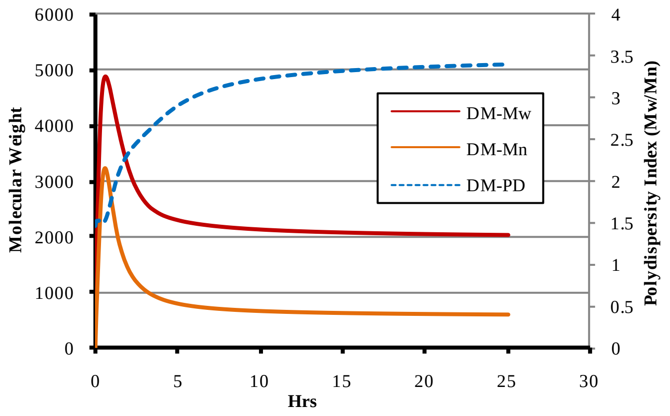

Figure (10) – The number average molecular weight (M_n), the weight average molecular weight (M_w), and the polydispersity index (PD = M_w/M_n) from the distributed model (DM) (Run 149). Rate constants from table (1) indicated by either "both" or "distrib"; max DP:100.

5.2.6 Lumped Model using Distributed Rate Constants; Far Off Conversion

The forward and reverse propagation rate constants differ significantly between the lumped model form and the distributed model form. Since the distributed model represents the kinetics exactly, the rate constants from that model (table (1) indicated by either "both" or "distrib") are closer to the true physical constants. The results from running the lumped model, with its depropagation to monomer, using the distributed model rate constants are shown in **Figure (11)**, compared to the distributed model and the Pruckmayr and Wu (1978) experiments. The trends are qualitatively similar to the lumped model with its own best fit constants (figure (1) and (2)), but the conversion is much lower, and the resulting M_n is also much lower.

This shows that the apparently small difference of including, or not, the reverse initiation reaction results in a significantly different system.

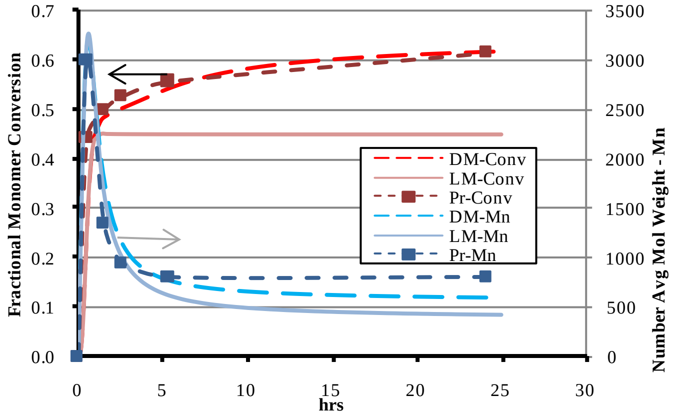

Figure (11) – Lumped model results (LM) (Run 1187) and distributed model results (DM) (Run 149; max DP:100) for THF Conversion and Mn compared to measurements of Pruckmayr and Wu (1978) (Pr) in 15.5 mol% CDCl3 (non-polar.) Both models use the best rate constants found for the distributed model from table (1) indicated by either "both" or "distrib".

5.2.7 Comparison to Brown and Szwarc (1958) Distribution

The formula of Brown and Szwarc (1958) (discussed above) predicts a simple geometric progression in the number fraction of chains as length increases. As discussed, the assumptions underlying that model don’t hold in this system. The MWD produced by the model is compared to the Brown and Szwarc (1958) prediction in **Figures (12) and (13)**. Brown and Szwarc (1958) formula depends on only one value: the fraction of chains of length 1. To compute that distribution, the value (=0.1815, Run 149) is taken from the distributed model. It’s important to note that, without the distributed model result, there would be no direct way of knowing that value or of calculating the distribution.

As Figure (12) shows, the number fraction distributions appear quite close. But the weight fraction distributions in Figure (13) reveal significant differences. As shown earlier in the lumped model results, a significant fraction of chains are terminated, thus fixing their lengths during the early part of the reaction when M_n is quite high. The result from this can be seen in the weight distribution, where the model shows a sustained contribution of polymer weight well into chain lengths near 100, while the Brown and Szwarc (1958) distribution is negligible above about 35. Termination of chains is not accounted for by the Brown and Szwarc (1958) formula. But termination very early in the reaction, when the transient elevated tail still exists in the few chain lengths at and below the maximum DP, is enough to cause a visible tail in the M_w distribution, and with a maximum DP of 100, the M_w distribution does not decrease to zero at DP=100.

The Brown and Szwarc (1958) formula has another inconsistency with this system. Their formula requires that the active dimer not reverse propagate to the active monomer. As shown earlier, including or excluding the reverse initiation reaction has a major impact on the conversion that is calculated, and this is because that error impacts the chains with the highest concentration. The active dimer restriction impacts the chains with the second highest concentration, so it seems likely that, even in the absence of the FSO_3^- reactions, their formula would not accurately predict the distribution in this system.

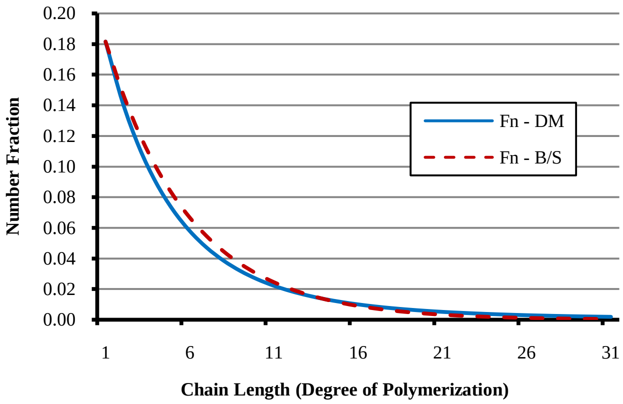

Figure (12) – Lower range of the number fraction of chains (Fn) from the distributed model results (DM) (Run 149) compared to the analytical distribution of Brown and Szwarc (1958) (B/S) ; max DP:100. Brown and Szwarc (1958) f_1 value (=0.1815) taken from the distributed model result. Distributed model rate constants from table (1) indicated by either "both" or "distrib".

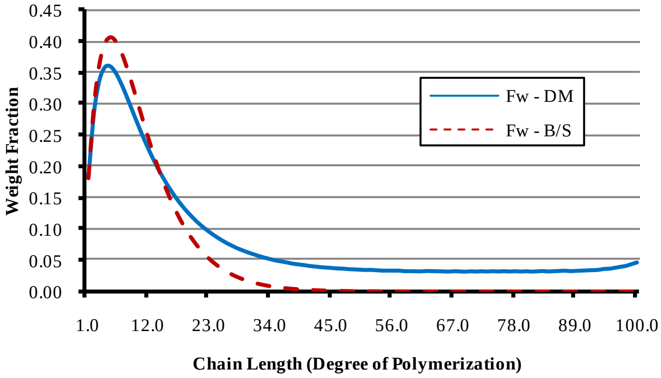

Figure (13) – Full range of the weight fraction of chains (Fw) from the distributed model results (DM) (Run 149) compared to the analytical distribution of Brown and Szwarc (1958) (B/S) ; max DP:100. Brown and Szwarc (1958) f_1 value (=0.1815) taken from the distributed model result. Distributed model rate constants from table (1) indicated by either "both" or "distrib".

6 Industrial Utility

FSA synthesis of PTMEG is an old technology. Still, about 20% of world capacity uses it, mostly in China. These smaller manufacturers can't justify the investment to license and build plants using the more sophisticated immobilized acid technology. Where capital is limited, improvements in the process, and hence business performance, must come from optimization. Even during business downturns, optimization remains a key tool for keeping a process profitable under lower capacity conditions; conditions that may differ from the design basis of the process. And where costly experiments or pilot plants were needed to develop the recipes and conditions for a product, models allow such experiments at low cost. These are applications in which the models in this study bring value.

Both the lumped and the distributed model are for a batch process. By simply adding flow in and out terms to the balances, these can be easily adapted to dynamic CSTR or semi-batch form. In that form, they can have great value for both for process and product design and optimization.

6.1 Flowsheet Optimization

Where larger process issues impact reactor operation, such as limited capacity in a downstream distillation column, potential solutions can be explored and developed by incorporating the lumped model into a flowsheet model. This can used to evaluate the interaction between reactor conditions, surrounding process unit capability, and product quality.

6.2 New Product Design

Potential new products, with different MWDs and hence end use properties, may be designed and process conditions indentified using the distributed model, with its high fidelity and its ability to predict MWD.

6.3 Control Study and Design

Since both models are dynamic, they can be used to study dynamic behavior. This can lead to changes in recipe and control strategy to address operating problems during upsets and transitions. The lumped model, with its modest size, could readily be integrated into a dynamic flowsheet model. It could provide valuable insight into changes in M_n with changing process conditions and lead to better control strategies. Though more challenging, the distributed model might also be integrated into a dynamic flowsheet model. This would open a new window into the changes in the complete MWD during transitions, upsets, and control moves in the process. Understanding how MWD changes during process changes, virtually impossible using lab measurements, could lead to control improvements and potentially even to narrow MWD products not now possible.

6.4 State Estimation and Control

Either model could be implemented as a real time state estimator. Rather than using fixed flows and compositions, these values can be retrieved from the real time process data measurements, and the model can be solved contemporaneously with the process itself. This provides an inferential estimate of the complete MWD, conversion, and side reaction products in the plant, continuously in real time. Such a state estimator can have two powerful uses.

First, it can improve yield to first grade product. Lab analyses are expensive, take a long time, and can't be done frequently. During process transitions or upsets, product may have to be partitioned ad hoc into different tanks, and subsequent lab analysis used to release or preprocess a whole tank. An estimator, by continuously indicating the MWD and other properties exiting the reactor, can show the precise moment when product moves back into spec and can be switched back to an in-spec product tank. Thus, only non-compliant product can be isolated, and all in-spec product can be sold.

Second, a state estimator can provide a continuous input to controls. Rather than running the reactor at fixed conditions, waiting for the next lab sample to be taken and analyzed, adjustments to reactor conditions can be made continuously, based on the state estimate. Then when the lab result becomes available and has been screened for variability, the baseline conditions can be adjusted if needed. Such estimator-based controls can significantly reduce variability, reduce off-spec product, and steer the process away from upsets.

All of these potential uses make sense in smaller plants in challenging business environments, because they can be implemented with no significant capital investment. In fact, because this model shows what MWD is formed, novel conditions can be simulated, potentially leading to new and different products. Given the difficulty of developing this model, it's quite possible that the immobilized acid manufacturers don't have such a predictive model for their technology. In that case, this model might lead to novel PTMEG products made by FSA synthesis that can't be produced in the immobilized acid synthesis, providing a competitive advantage and potentially extending the life and value of the FSA synthesis.

7 Conclusion

By carefully studying the work of polymer chemists, considering all the evident reactions that can take place, and working meticulously to model the many polymer species that can arise, a full dynamic prediction of the MWD is possible for the FSA initiated synthesis of PTMEG. Even though PTMEG has been manufactured by FSA initiation for decades and numerous chemistry studies were published, the work presented here appears to be the first published model to produce both bulk properties and molecular weight distribution.

The FSO_3^- counter ion reactions with both ends of active chains, terminating chains and transferring activity back to initiator, are key to getting the correct results. The reversibility of this polymerization results in a significant spike in M_n early in a batch reaction, and these reactions freeze chains. This leaves a significant fraction of longer chains which were terminated early in the reaction, and shifts the distribution away from the geometric shape predicted by Brown and Szwarc (1958). These long chains have a large impact on M_w and thus on end product properties.

The previously published rate constants were derived using a lumped model, which doesn’t properly represent the chemistry in this system, so the constants derived here and presented in table (1) as "both" or "distrib" correspond to the rates of the reactions that are actually taking place in this system. The lumped model, though not accurate in the conversion vs. time profile, predicts M_n fairly well and still may have value as a plug-in for larger flowsheet studies. The detailed distributed model closely matches all the measured bulk properties and gives a full molecular weight distribution.

Both the lumped and distributed models can be easily adapted to semi-batch or CSTR form. Either as modeling study tools or real-time estimators, they enable new product design, process control studies, new process design, process optimization and control, and reduction of product variability and waste – all not previously possible.

Acknowledgments: My thanks to Thomas Keane (DuPont Fellow, Ret), Eric Grulke (Univ of Kentucky), P David Schnelle (DuPont Engineering), PC Gopalratnum (Invista), and Elyssa Skeirik (Georgetown Univ) for their review of and suggestions for the manuscript.

Table (1): Best rate constants found for the lumped model representation (Lump) (Run 86) and the distributed model representation (Distrib) (Run 149). Only the forward initiation and forward and reverse propagation constants differ between the two model representations. The other constants are the same in both (Both) representations.

Equation	Description	Forward/Reverse	Model	Value	Units
(8)	FSA Dissociation	Forward	Both	0.65	hr^{-1}
		Rev	Both	.012	$l \cdot mol^{-1} \cdot hr^{-1}$
(9)	HF Association	Forward	Both	0.00	hr^{-1}
		Rev	Both	90.0	$l \cdot mol^{-1} \cdot hr^{-1}$
(10)	Initiation	Forward	Lump	0.18	$l \cdot mol^{-1} \cdot hr^{-1}$
		Forward	Distrib	0.12	$l \cdot mol^{-1} \cdot hr^{-1}$
		Rev	Both	0.0	hr^{-1}
(11)	Propagation	Forward	Lump	19.8	$l \cdot mol^{-1} \cdot hr^{-1}$
		Forward	Distrib	62.5	$l \cdot mol^{-1} \cdot hr^{-1}$
		Rev	Lump	85.3	hr^{-1}
		Rev	Distrib	400.	hr^{-1}
(12)	FSO_3^- attack on OH	Forward	Both	100.	$l \cdot mol^{-1} \cdot hr^{-1}$
		Rev	Both	0.00	hr^{-1}

(13)	FSO$_3^-$ attack on $^+$THF	Forward	Both	0.50	$\mathrm{l \cdot mol^{-1} \cdot hr^{-1}}$
		Rev	Both	0.00	$\mathrm{hr^{-1}}$
(14)	FOSO$_2$ attack on OH	Forward	Both	112.	$\mathrm{l \cdot mol^{-1} \cdot hr^{-1}}$
		Rev	Both	0.00	$\mathrm{hr^{-1}}$
(15)	HOSO$_3$ attack on $^+$THF	Forward	Both	0.90	$\mathrm{l \cdot mol^{-1} \cdot hr^{-1}}$
		Rev	Both	0.00	$\mathrm{hr^{-1}}$

8 References

Balster A.E., Komarov V.M., Bazanov A.G., Zubritskaya N.G., Machalaba N.N., 2011. Effect of the Basic Process Parameters During Polymerization of Tetrahydrofuran with Perchloric Acid. Fibre Chemistry 42 215-219.

Brown W.B., Szwarc M., 1958. Molecular Weight Distribution of "Living" Polymers. Transactions of the Faraday Society 54 416-419.

Bryner M., 2007. DuPont Develops New Family of Renewable Polymers. Chemical Week, Jun 13 2007 p 12.

Chemical Week, 1999. Penn Selects Lyondell THF Technology. Jul 21 1999 20.

Chemical Week, 2010. Invista Licenses Technology...Plans to Upgrade Texas Plants. Nov 8/15 2010 p 30.

China Chemical Reporter, 2005. PTMEG Project Startup in Jilin. Aug 26 2005 p 14.

China Chemical Reporter, 2010. Spandex Goes into Oversupply. July 6 2010 p 28.

Dorai S., Pruckmayr G., Marsi M., Quon W., 1992. Polymerizing Tetrahydrofuran to Produce Polytetramethylene Ether Glycol using a Modified Fluorinated Resin Catalyst containing Sulfonic Acid Groups. (E. I. Du Pont de Nemours and Co.) US 5118869.

Flory P.J., 1936. Molecular Size Distribution in Linear Condensation Polymers. J American Chemical Society 58 1877-1885.

IHS Chemical Week 2012. BASF Invests $75 Million to Increase PolyTHF Capacity. Aug 27/Sept 3 2012 p 4.

Kobayashi S., Danda H., Saegusa T., 1973. Kinetic Studies on the Cationic Ring-Opening Polymerization of Tetrahydrofuran Initiated by Superacid Esters. Bulletin of the Chemical Society of Japan 46 3214-3220.

Mueller H., Huchler O.H., Hoffman H., 1980. Polymerization of tetrahydrofuran (BASF AG) US 4189566.

Mueller P.A., Richards J.R., Congalidis J.P., 2011. Polymerization Reactor Modeling in Industry. Macromolecular Reaction Engineering 5 261-277.

Paint & Coatings Industry Magazine, 2002. Lyondell Chemical Co. 18(10) 28.

Pruckmayr G., Dreyfuss P., Dreyfuss M. P., 2000. Polyethers, Tetrahydrofuran and Oxetane Polymers, in Kirk-Othmer Encyclopedia of Chemical Technology, Wiley, New York .

Pruckmayr G., Wu T.K., 1978. Polymerization of Tetrahydrofuran by Proton Acids. Macromolecules 11, 662-668.

Saegusa T., 1972. Polymerization of Cyclic Ethers. J Macromolecular Science - Chemistry A6 997-1026.

Zejiang L., Hui S., 2010. Maleic Anhydride Production in China. China Chemical Reporter Dec 21 2010 p 14-16.

Figure Captions

Figure (1) – Lumped Model (LM) Simulation: Number average molecular weight (M_n) and THF Conversion (Run 86) compared to measurements of Pruckmayr and Wu (1978) (Pr) in 15.5 mol% $CDCl_3$ (non-polar.) Rate constants from table (1) indicated by either "both" or "lump". Dashed lines are interpolated.

Figure (2) – Lumped Model (LM) Simulation: Fraction of Fluorine in 3 forms (Run 86); compared to F-NMR measurements of Pruckmayr and Wu (1978) (Pr) in 20 mol% CH_2Cl_2 (non-polar.) OSO_2F is alkyl fluorosulfate. Rate constants from table (1) indicated by either "both" or "lump". Dashed lines interpolated. Distributed model results are effectively equivalent.

Figure (3) – Lumped Model (LM) Simulation: Fraction of sulfur in 2 forms: alkyl sulfate (AS) and dialkyl sulfate (DAS); compared to H-NMR measurements of Pruckmayr and Wu (1978) (Pr) in 15.5 mol% $CDCl_3$ (non-polar.) Rate constants from table (1) indicated by either "both" or "lump". Dashed lines interpolated. Distributed model results are effectively equivalent.

Figure (4) – Lumped Model (LM) Simulation (Run 99) showing the integral concentration of chains activated, terminated by FSO_3^-, terminated by alkyl sulfate (AS); and the instantaneous number of active chains (Live) $mol \cdot l^{-1}$; and the number average molecular weight (M_n - right hand scale).

Figure (5) – Lumped model (LM) results (Run 86) and distributed model (DM) results (Run 150) for THF Conversion and M_n compared to measurements of Pruckmayr and Wu (1978) (Pr) in 15.5 mol% $CDCl_3$ (non-polar.) Rate constants in both models are best lumped values from table (1) indicated by either "both" or "lump". Dashed lines interpolated.

Figure (6) – Lumped model results (LM) (Run 86) and distributed model results (DM) (Run 149) for THF Conversion and M_n compared to measurements of Pruckmayr and Wu (1978) (Pr) in 15.5 mol% $CDCl_3$ (non-polar.) Each model uses its own best fit rate constants from table (1); lumped indicated by "lump" and distributed indicated by "distrib". Dashed lines interpolated.

Figure (7) – Distributed model result (Run 149) for total concentration of polymer chains and equivalent concentration of monomer already reacted to form polymer; mol·l-1 . Rate constants from table (1) indicated by either "both" or "distrib".

Figure (8) – Molecular weight distribution (MWD) summing all chains with same DP regardless of end groups (Run 149) early in the reaction; mol·l^{-1} . The elevated tails arise briefly when chains longer than 100 have significant concentration. Rate constants from table (1) indicated by either "both" or "distrib"; max DP:100.

Figure (9) – Lower range of the molecular weight distribution (MWD) summing all chains regardless of end groups (Run 149) later in the reaction; mol·l^{-1} . The concentration axis scale is 15 times that of Figure (8). Rate constants from table (1) indicated by either "both" or "distrib"; max DP:100.

Figure (10) – The number average molecular weight (M_n), the weight average molecular weight (M_w), and the polydispersity index (PD = M_w/M_n) from the distributed model (DM) (Run 149). Rate constants from table (1) indicated by either "both" or "distrib"; max DP:100.

Figure (11) – Lumped model results (LM) (Run 1187) and distributed model results (DM) (Run 149; max DP:100) for THF Conversion and Mn compared to measurements of Pruckmayr and Wu (1978) (Pr) in 15.5 mol% CDCl3 (non-polar.) Both models use the best rate constants found for the distributed model from table (1) indicated by either "both" or "distrib".

Figure (12) – Lower range of the number fraction of chains (Fn) from the distributed model results (DM) (Run 149) compared to the analytical distribution of Brown and Szwarc (1958) (B/S) ; max DP:100. Brown and Szwarc (1958) f_1 value (=0.1815) taken from the distributed model result. Distributed model rate constants from table (1) indicated by either "both" or "distrib".

Figure (13) – Full range of the weight fraction of chains (Fw) from the distributed model results (DM) (Run 149) compared to the analytical distribution of Brown and Szwarc (1958) (B/S) ; max DP:100. Brown and Szwarc (1958) f_1 value (=0.1815) taken from the distributed model result. Distributed model rate constants from table (1) indicated by either "both" or "distrib".

Schema (1) – Reactions used in the model. Only the reactions of equation (8) and (11) are reversible. HF does not dissociate in this system.